Effect of Gap Junction Uncoupling on Spatial Dispersion of Action Potential Duration at Sites of Abrupt Tissue Expansion

Marjorie Letitia Hubbard, Craig S Henriquez

Duke University, Durham, USA

Abstract

Spatial dispersion of action potential duration has been linked to arrhythmogenesis in the diseased heart; however, the complex dynamic between repolarization dynamics and microstructural heterogeneity in critical regimes is largely unknown. The objective of this study was to use microstructural computer models of adult monolayers to study the effect of abrupt tissue expansion and gap junction uncoupling on dispersion of action potential duration (APD) during premature stimulation. Two-dimensional discrete and equivalent continuous computer models (dx=10 µm, dy=10 µm) of ventricular monolayers with isthmus strands connected to a load region were generated. In the discrete model, gap junctions (g_j) with a value between 0.005 µS and 0.50 µS were uniformly distributed around individual cells. In strands with a width of 300 µm, decreasing gap junction coupling in the discrete model increased variation in APD at the site of abrupt expansion by as much as 6 ms and changed the APD profile at the expansion site from an elliptical to a bipolar configuration. In narrow strands with a width of 60 µm, uniformly decreasing coupling in both the strand and the load increased variation in APD by as much as 14 ms and facilitated propagation at the expansion site. The equivalent continuous model could not reproduce microstructural variations in APD, the pattern of conduction block observed in moderately coupled tissue or the conduction delay observed at the site of abrupt expansion.

1. Introduction

Arrhythmogenesis in the diseased heart has been linked to spatial dispersion of repolarization[1,2]. While a number of experimental studies have focused on electrophysiological or pacing mechanisms leading to spatial dispersion of repolarization, only a few studies have investigated the impact of pathological changes in cardiac structure on heterogeneity in action potential duration (APD)[3,4]. A systematic computational modeling study by Fenton and Cherry has demonstrated that source-sink imbalances caused by stimulation, physical boundaries, and tissue geometry can lead to spatial variations in APD as large as tens of milliseconds[5]. One recent experimental and computational study in patterned monolayers showed that tissue narrowing and expansion similar to that observed in diseased tissue can prolong the action potential plateau at the expansion site leading to wavefront reflection and functional reentry[6].

Using 1-D and 2-D microstructural models of adult monolayers, Hubbard and Henriquez have shown that abrupt changes in coupling can also lead to spatial variations in action potential duration, and these studies suggest that in critical regimes near the onset of conduction block, variations in cardiac microstructure may lead to more complex spatial distributions of action potential duration and conduction block that facilitate wavefront reentry [7,8]. The objective of this study was to use microstructural computer models of adult monolayers to study the effect of abrupt tissue expansion on dispersion of action potential duration (APD) during premature stimulation in well-coupled and poorly coupled tissue.

2. Methods

Two-dimensional microstructural computer models (dx=10 µm, dy=10 μm) of ventricular monolayers that incorporated discrete, uniformly distributed gap junctions (g_j) were randomly generated using methods previously described [9]. The individual myocytes were an average

Figure 1. Tissue model with an isthmus with discrete microstructure shown at the abrupt expansion.

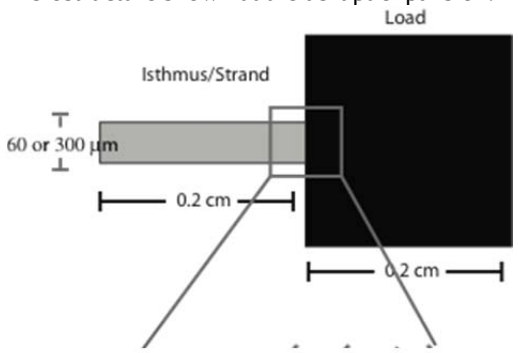

of 100 μm in length and 30 μm in width. Isthmus strands of variable width (Narrow: 60 μm or Wide: 300 μm) were connected to a larger cell area that was 0.20 cm x 0.20 cm as shown in Figure 1.

Gap junction conductance within the strand and the larger cell area was uniformly set to 0.50 μS (well-coupled tissue), 0.05 μS (moderately coupled tissue) and 0.005 μS (poorly coupled tissue). In each case, two randomly generated inhomogeneous tissue models representing different realizations of the same microstructure statistics (cell shape, size, coupling) were created in order to test the sensitivity of the results to random changes in tissue architecture. A modified LRD model of guinea pig ventricular tissue was used to simulate the ionic properties.

Equivalent continuous models (dx=10 μm, dy=10 μm) with uniform resistive properties were created by adjusting the resistivity of the continuous model to match the longitudinal and transverse conduction velocities measured in a 0.40x0.40cm discrete tissue model with no isthmus. Three stimuli (S1S2S3) were given at the left boundary of the isthmus strand at a basic cycle length (BCL) of 200 ms.

All simulations used the CardioWave software platform[10]. A semi-implicit scheme with a conjugate gradient solver was used to solve the system of equations. The time step was kept constant at 5 μs, output data were recorded every 10 μs, and the data for the activation and recovery maps were recorded at a minimum of every 100 μs. Action potential duration was measured at 85% repolarization.

3. Results

3.1. Wide isthmus (300 μm)

Well-coupled (g_j=0.50 μS)

In well-coupled strands with a width of 300 μm, APD declined from 179 to 177 ms as the first wavefront propagated toward the abrupt expansion and then declined more steeply to 174 ms as the wavefront propagated away from the site of abrupt expansion toward the tissue boundary. After the second beat, APD approached 124 ms in the center of the strand and then declined to 120 ms as the wavefront approached the tissue boundary. In both cases, the shape of the APD profile in the load region was elliptical and no significant increase in APD was observed at the abrupt expansion.

Moderately coupled (g_j=0.05 μS)

In moderately coupled strands, the 2-D APD profile as the first wavefront exited the strand was no longer elliptical, with the lowest APD (176 ms) occurring in the center of the strand and higher APD (177 ms) occurring at the outermost borders of the abrupt expansion. As the wavefront approached the tissue boundary, APD declined to 172 ms. After the second beat, APD reached a minimum of 121 ms in the center of the strand and a maximum APD of 123 ms at the outermost boundary of the abrupt expansion. APD declined to 119 ms as the wave approached the tissue boundary.

Poorly coupled (g_j=0.005 μS)

The variation in APD profile was more pronounced in poorly coupled tissue (Figure 2A), with APD after the first beat increasing from 173 ms in the center of the strand to 175 ms, at the site of abrupt expansion. The maximum APD of 177 ms (excluding the stimulus site) occurred in single cells near the outermost corners of the expansion. As the wavefront approached the tissue boundary, APD declined to 169 ms. After the second beat, the APD increased from 121 ms within the strand to 125 ms at the center of the abrupt expansion, with a localized maximum of 127 ms near the corner of the abrupt expansion. APD in the load region gradually increased to 127 ms along the transverse direction, before rapidly declining to 123 and 121 ms near the transverse and longitudinal tissue boundaries, respectively.

Continuous equivalent

Continuous well-coupled and moderately coupled tissue had the same APD profile as observed in discrete tissue. In poorly coupled continuous tissue (g_j=0.005 μS), APD at the abrupt expansion (174 ms) showed no significant increase in APD compared to the center of the strand after the first beat. APD increased to 176 ms at the outermost edges of the expansion site (Figure 2B). After the second beat, APD increased from 121 ms in the center of the strand to 123 ms at the abrupt expansion. In contrast to discrete tissue, individual cells with localized increases in APD were not observed near the corners of the abrupt expansion, and there was very little variation in APD after the second beat (Figure 2B).

3.2. Narrow isthmus (60 μm)

Well-coupled (g_j=0.50 μS)

In well-coupled models (g_j=0.50 μS), propagation blocked for all three stimuli given at a BCL of 200 ms. The maximum APD reached in the strand prior to block was 64 ms.

Moderately coupled (g_j=0.05 μS)

In moderately coupled tissue models with a strand width of 60 μm, APD after the first beat increased from 177 ms within the strand to maximum of 180 ms at the site of abrupt expansion. APD declined to 173 ms as the wave approached the tissue boundary. The second beat blocked at the expansion site. The maximum APD reached in the strand prior to block was 98 ms.

Figure 2. A) APD maps taken after the first beat and a second beat given at 200ms in *discrete* poorly coupled tissue with a 300 µm isthmus B) APD maps taken after the first second beat in *equivalent continuous* tissue with a 300 µm isthmus.

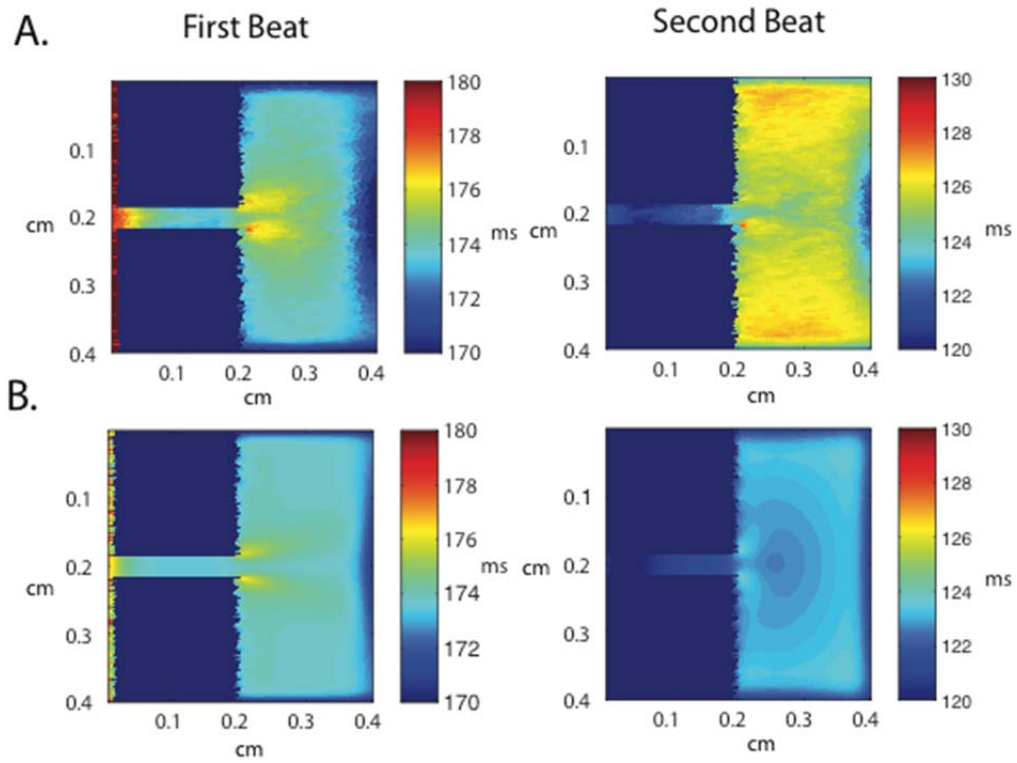

Poorly coupled (g_j=0.005 µS)

In poorly coupled tissue models with a width of 60 µm, APD after the first beat increased from 174 ms within the strand to maximum of 182 ms, a difference of 8 ms, at the site of abrupt expansion. As the wavefront approached the tissue boundary, APD declined to 169 ms. After the activation of the second beat, APD flattened out at 120 ms in the center of the strand and increased to 134 ms as the wavefront approached the abrupt expansion, a difference of 14 ms. Within the load region, the APD flattened out at 128 ms before declining steeply to 124 ms as the wavefront approached the tissue boundary. In both cases the shape of the APD profile in the load region was elliptical.

Continuous equivalent

In well-coupled equivalent continuous models (g_j=0.50 µS), propagation also blocked for all three stimuli given at a BCL of 200 ms.

In the moderately coupled equivalent continuous models (g_j=0.05 µS), all three beats were able to propagate from the strand to the load. This is in contrast to the discrete case in which the second beat blocked at the expansion site. The conduction delay at the transition from the strand to the load was much less pronounced in the continuous tissue (Figure 3A) compared to the discrete tissue (Figure 3B).

Similarly to poorly coupled discrete models (g_j=0.005 µS), all three beats were able to propagate from the strand into the load in poorly coupled continuous models; however, the maximum APD at the abrupt expansion after the first beat in the continuous strand was 177 ms compared to a maximum of 182 ms in the discrete strand. The maximum APD in the continuous tissue after the second beat was 124 ms compared to 134 ms in discrete tissue.

4. Conclusions

At the abrupt expansion, there is a mismatch in repolarizing current that leads to increased APD as the wavefront exits the strand into the load region[11]. In tissue with a wide strand, reducing coupling causes the APD profile at the abrupt expansion to change from a single elliptical shape to two individual ellipses at the edges of the abrupt expansion. The increases in APD caused by microstructure are most pronounced at the corners of abrupt expansions and along the transverse axis. Equivalent continuous models do not completely capture the microstructural variation in APD near the abrupt expansion, which can lead to very different APD responses to a second premature beat.

As the width of the strand narrows, the wavefront becomes more likely to fail as it exits the abrupt expansion[12]. Uniformly decreasing intercellular coupling reduces the effect of the load region on APD,

Figure 3. Action potential propagation from a narrow strand to a larger load after the first beat in A) discrete tissue (gj=0.05 μS) and B) equivalent continuous tissue.

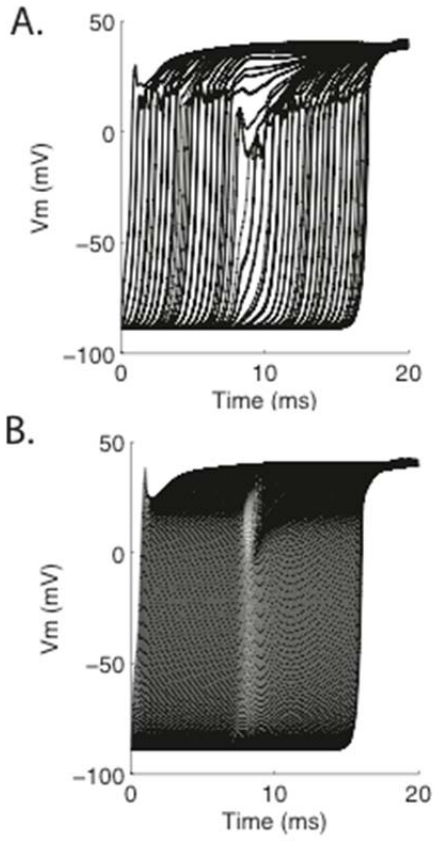

thus facilitating conduction; however, it also enhances variations in APD caused by structural microheterogeneity at the expansion site [13]. In moderately coupled tissue, the decrease in the load does not always balance the increase in APD at the expansion caused by decreased coupling, leading to conduction block when a premature stimulus reaches the expansion site while the tissue is still refractory. Continuous models do not completely capture the dynamics of propagation and conduction delay at the abrupt expansion close to failure, which can lead to very different response to a second premature beat compared to discrete models.

Future studies will systematically investigate the effect of microstructure on action potential dispersion for a range of excitation frequencies, coupling levels, and strand properties in both discrete and continuous tissue models. Additional studies will also focus on the effect of microstructural variations in action potential duration on the formation of complex patterns of activation in ectopically active tissue

References

[1] Han J, Moe GK. Nonuniform recovery of excitability in ventricular muscle. Circ Res 2001; 87:E25-E36.

[2] Antzelevitch, C. Role of spatial dispersion of repolarization in inherited and acquired sudden death syndromes. Am J Physiol Heart Circ Physiol 2007; 293:H2024-H2038.

[3] Sampson K, Henriquez CS. Interplay of ionic and structural heterogeneities on functional action potential gradients: Implications for arrhythmogenesis. Chaos 1999;12:821-4.

[4] Sampson K, Henriquez CS. Simulation and prediction of functional block in the presence of structural and ionic heterogeneity. Am J Physiol Heart Circ Physiol 2001; 281: H2597-2603.

[5] Fenton F, Cherry E. Effects of boundaries and geometry on the spatial distribution of action potential duration in cardiac tissue. J Theor Biol 2011; 285(1):164-76.

[6] Auerbach A, Grzeda K, Furspan P, Sato P, Mironov S, Jalife J. Structural heterogeneity promotes triggered activity, reflection and arrhythmogenesis in cardiomyocyte monolayers. J Physiol 2011; 589:2363-81.

[7] Hubbard ML and Henriquez CS. Increased interstitial loading reduces the effect of microstructural variations in cardiac tissue. Am J Physiol Heart Circ Physiol 298: H1209-1218, 2010.

[8] Hubbard ML and Henriquez CS. Microscopic variations in interstitial and intracellular structure modulate the distribution of conduction delays and block in cardiac tissue with source-load mismatch. Europace 14: v3-v9, 2012.

[9] Hubbard ML, Ying W, and Henriquez CS. Effect of gap junction distribution on impulse propagation in a monolayer of myocytes: a model study. Europace 9: vi20-28, 2007.

[10] Pormann J. A modular simulation system for the bidomain equations. PhD Thesis. Duke University Department of Electrical and Computer Engineering, 1999.

[11] Steinhaus BM, Spizer KW, Isomura S. Action potential collisioni in heart tissue. Computer simulations and tissue experiments. IEEE Trans Biomed Eng 1985; 32:731-742.

[12] Cabo C, Pertsov AM, Baxter WT, Davidenko JM, Gray RA, Jalife J. Wavefront curvature as a cause of slow conduction and block in isolated cardiac muscle. Circ Res 1994; 75:1014-28.

[13] Rohr S, Kucera J.P, Fast V.G, Kléber A.G. Paradoxical improvement of impulse conduction in cardiac tissue by partial cellular uncoupling. Science 1997; 275:841–844.

Address for correspondence.
Marjorie Letitia Hubbard
Duke University
Department of Biomedical Engineering
136 Hudson Hall
Durham, NC 27704
mlh23@duke.edu